Multi-GNSS Constellation Anomaly Detection and Performance Monitoring

Kazuma Gunning, *Stanford University*
Todd Walter, *Stanford University*
Per Enge, *Stanford University*

BIOGRAPHIES

Kaz Gunning is a Ph.D. candidate in the GPS Research Laboratory working under the guidance of Professor Per Enge and Dr. Todd Walter in the Department of Aeronautics and Astronautics at Stanford University. Prior to joining the lab in fall 2015 as a Ph.D. candidate, Kaz worked for Booz Allen Hamilton on the GPS Systems Engineering and Integration group doing Modeling and Simulation of the next generation GPS Control Segment and software-defined receiver work looking at the GPS III waveform. His interests are in GNSS modernization and integrity.

Todd Walter is a senior research engineer in the GPS Research Laboratory in the Department of Aeronautics and Astronautics at Stanford University. He received his Ph.D. from Stanford in 1993 and has worked extensively on the Wide Area Augmentation System (WAAS). He is currently working on dual-frequency, multi-constellation solutions for aircraft guidance. He received the Thurlow and Kepler awards from the ION. In addition, he is a fellow of the ION and has served as its president.

Per Enge is a Professor of Aeronautics and Astronautics at Stanford University, where he is the Vance and Arlene Coffman Professor in the School of Engineering. Here, he directs the GPS Research Laboratory which develops navigation systems based on the Global Positioning System (GPS). He has been involved in the development of WAAS and LAAS for the Federal Aviation Administration (FAA). He has received the Kepler, Thurlow, and Burka Awards from the ION. He also received the Summerfield Award from the American Institute of Aeronautics and Astronautics (AIAA) as well as the Michael Richey Medal from the Royal Institute of Navigation. He is a fellow of the Institute of Electrical and Electronics Engineers (IEEE), a fellow of the ION, a member of the National Academy of Engineering, and has been inducted into the Air Force GPS Hall of Fame. He received his Ph.D. from the University of Illinois in 1983.

ABSTRACT

This paper describes a process by which Global Navigation Satellite System (GNSS) nominal statistics and fault rates can be assessed with high confidence. The use of a GNSS in Advanced Receiver Autonomous Integrity Monitoring (ARAIM) requires knowledge of the level of performance of the signal-in-space (SIS) user range error (URE) in both nominal and faulty conditions. The performance characterization is done through a careful analysis of historical data, from which a determination of whether or not it meets the performance commitments of the constellation service provider (CSP) can be made. Typically, this analysis is carried out though a comparison of the broadcast navigation messages with post-processed precise estimates of the satellite clock and orbit states. This paper highlights the issues with such an approach as well as mitigation strategies to those issues. The issues primarily impact the estimates of fault rates rather than nominal statistics, as the number of faults is small compared to the overall amount of nominal data. In particular, methods of ensuring integrity in the logged broadcast navigation messages and precise clock and orbit products used in the analysis are described.

In order to verify precise clock and orbit products, a Kalman filter (KF) to produce independent GNSS clock bias estimates has been developed and tested. The KF leverages the International GNSS Service (IGS) receiver network to produce estimates of GNSS clock biases given precisely known positions of the receivers as well as precise satellite orbit products. The KF serves multiple purposes in detecting and verifying faults. First, when only low rate (5 or 15 minute) clock products are available, higher rate products can be produced to detect short faults. Second, when precise clock products are available, the KF serves as a secondary check to protect against erroneous external precise products, which have been observed. Initial testing of the filter has shown an RMS error of under 20 centimeters for a five day run of GPS clock bias estimates, which is sufficient performance for precise product verification and fault detection.

INTRODUCTION

Advanced Receiver Autonomous Integrity Monitoring (ARAIM) requires careful, long-term statistical quantification of the performance of the Global Navigation Satellite Systems (GNSS) that it leverages. This paper describes a system for anomaly detection, performance evaluation, and statistic generation for four core constellations: the Global Positioning System (GPS), Galileo, GLONASS, and BeiDou. The primary goal of the system is to quickly identify anomalous behavior caused by either the behavior of GNSS satellites or the Constellation Service Provider (CSP) and automatically notify researchers when such events are detected. Anomalous behavior due to satellite behavior might consist of a change in the rate of the atomic frequency standard (AFS) onboard the satellite that is not accompanied by a corresponding change in the broadcast clock bias and clock drift. Errors caused by the CSP more directly could consist of erroneous navigation data being uploaded and broadcast or incorrect health status being broadcast during an onboard clock reset or orbital maneuver. The secondary goal is long term characterization of constellation performance. Of particular interest are statistics related to the ARAIM Integrity Support Message (ISM): P_{sat} (probability of satellite fault), P_{const} (probability of constellation fault), and the bounding User Range Accuracy (URA) sigmas. Previous studies have characterized nominal performance and estimated P_{sat} and P_{const} for GPS [1, 2] and GLONASS [3], characterized nominal performance of Galileo [4] and BeiDou [5], or taken a multi-GNSS approach [6]. However, many of these studies are vulnerable to the errors that will be described in this paper.

This paper describes a system that uses multiple methods of evaluating ranging performance and detecting faults. The first method compares precise estimates of GNSS clock and orbital states provided by the IGS Multi-GNSS Experiment and Pilot Project (MGEX) analysis centers (AC) and the National Geospatial-Intelligence Agency (NGA) to the propagated broadcast navigation messages from each satellite. The broadcast navigation messages are found by compiling navigation message logs from individual GNSS receivers from the global IGS network and performing a voting algorithm on in order to screen out logging errors and best identify the navigation message that was applicable at each time. The precise and broadcast clock and ephemeris errors are combined to produce the signal-in-space (SIS) user range error (URE) and are compared against constellation-specific fault criteria. Our previous papers have done such an analysis for GPS and GLONASS over long periods, but these analyses were done in a more manual manner than the automated process described here.

This method is excellent at characterizing GNSS nominal performance, but multiple threats can introduce errors into the fault rate calculations. The rest of the paper describes the threats as well as mitigation strategies. The first threat is missing or erroneous broadcast navigation data, and both the threat and a mitigation strategy are described.

Similarly, precise clock and orbit estimates are not available at all times, whether because they have not produced yet or because there are simply missing periods in past precise clock and ephemeris products. The second part of this paper briefly describes how in these cases, one can identify faults using only the broadcast navigation data and the receiver network observation data. One can estimate the user range error (URE) of the satellite of interest and compare it to the fault criteria given by the CSP.

The final section of this paper describes a Kalman filter based system for producing independent GNSS clock bias estimates to verify external precise clock estimates and fill in when third-party estimates are unavailable. Using known locations of IGS receivers and the precise estimates of GNSS orbits, satellite and receiver clocks can be simultaneously estimated at 30 second intervals- a higher rate than the precise clock and ephemeris products directly available from the MGEX project. The system is described and initial results are presented.

Using all of these methods, we produce an analysis of constellation performance with much better availability than if one were to only use the precise ephemerides without the observation data.

Broadcast navigation message performance evaluation procedure

A more detailed depiction of the navigation message performance evaluation procedure is shown in Figure 1. The process, automatically performed on a daily basis, is initiated by first downloading data and products from the IGS and NGA FTP servers. The IGS and NGA provide precise estimates of GNSS orbit and clock states. IGS MGEX products and data are leveraged because many of the orbit and clock solutions comprise all four core GNSS constellations. The four primary types of data downloaded are MGEX precise orbit and clock solutions, MGEX higher rate precise clock solutions, NGA GPS orbit and clock solutions referenced to the satellite antenna phase center, and RINEX navigation message files from the receivers in the MGEX network. The system checks for new products that are available and downloads.

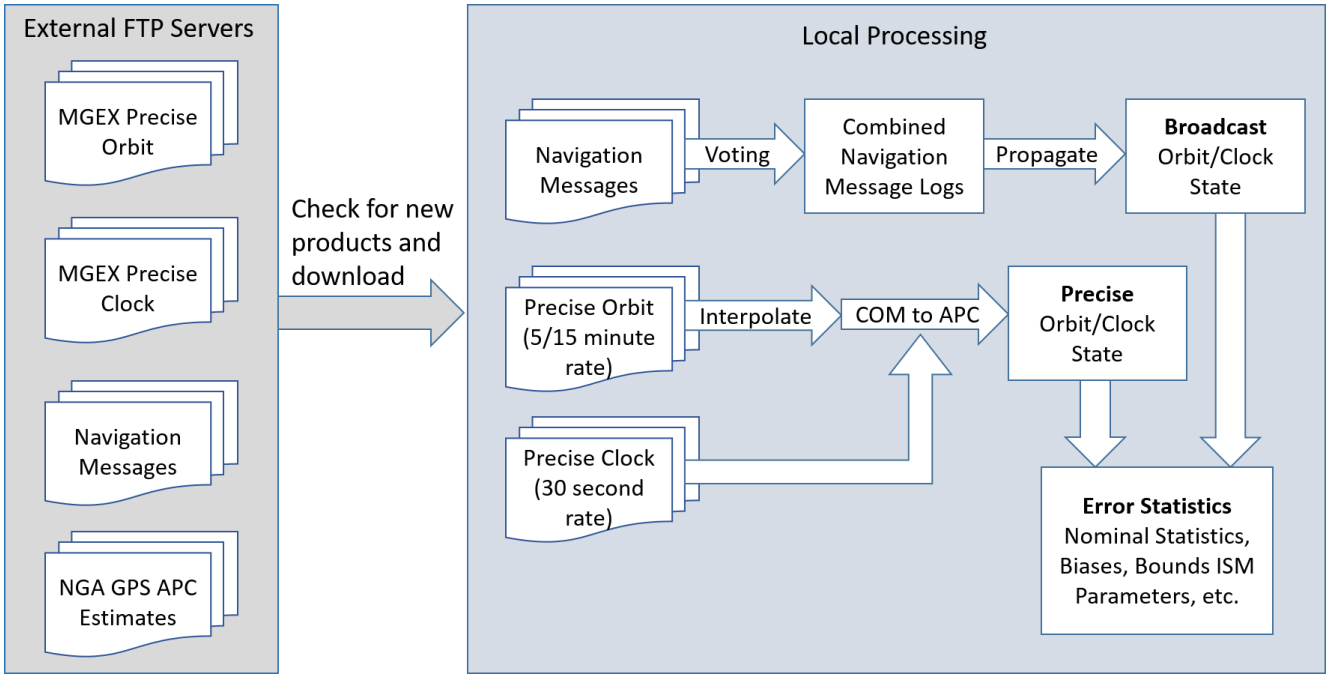

Figure 1: Broadcast navigation message performance evaluation process flow

Locally, the process starts by cleaning, voting on, and aggregating the receiver broadcast navigation message files into a single clean set of navigation messages per constellation per day. This process is described in more depth in the following section. For each desired epoch and satellite, the appropriate broadcast message is selected and propagated to the desired time. Special care is taken to ensure that the message should in fact be used by making sure to not use navigation messages out of their specified validity intervals and checking the broadcast health/URA/SISA. This propagated state is the broadcast orbit and clock state that will be used to compare against the precise data, where there is a broadcast state propagated for each available precise clock estimate.

The precise orbit estimates typically are produced with 5 or 15 minutes between consecutive estimates, while the precise clock estimates often go down to 30 second intervals. In order to match the two data sets, a Lagrange interpolation scheme is used to interpolate the orbit data to match the clock [7]. Additionally, the IGS orbit estimates refer to the center of mass of the satellites, while the broadcast ephemeris refers to the antenna phase center. The IGS estimates of antenna phase center offset [8] as well as a nominal yaw-attitude model [9] are used to translate from center of mass to antenna phase center.

At each desired epoch, the matching precise and broadcast clock and ephemeris states can be compared, or it can be noted that one or both of them is missing, and the reason for the missing data can be explored. The difference is taken between the two states, and statistics are produced. Many of the exact statistics have been described in depth in previous papers by Walter [1, 2] and Heng [10].

A few examples of the products produced through this process are shown in Figure 2Figure 4. The first example, Figure 2, shows an overview of the history of the GPS constellation from 2008-2017. Each horizontal line indicates the status of each satellite over time, whether it is healthy and unfaulted, in a faulted state, unhealthy, or whether there is missing precise data, broadcast data, or both. Figure 3 shows a subset of the nominal statistics produced for Galileo from 2015-2017. For each satellite, the broadcast navigation message error is broken down into clock and orbit error, with orbit error further broken down into the radial, along-track, and cross-track error. The black line marks the mean error, the green bar marks the 68% bounding, and the red bar marks the 95% bounding. The final example, in Figure 4, is of a clock and ephemeris anomaly that was observed in May 2017. The maximum projected user range error (MPE), indicated by the black line, is a primary metric used to compare against the fault threshold, which is indicated by the blue line. The MPE slowly drifts over the fault threshold and reaches 25 meters while entering a faulted state. The satellite then begins to broadcast an unhealthy status, and the

broadcast orbit and clock estimate is updated, but again the MPE drifts to nearly 40 meters over the course of the next day again.

These products, in addition to others including fault rate estimates and other ISM parameters, have been produced for all four core GNSS constellations up to the present. GPS data has been processed from 2008 on, GLONASS data has been processed from 2009 on, and Galileo and BeiDou have less data processed, from 2015 and 2016 on respectively.

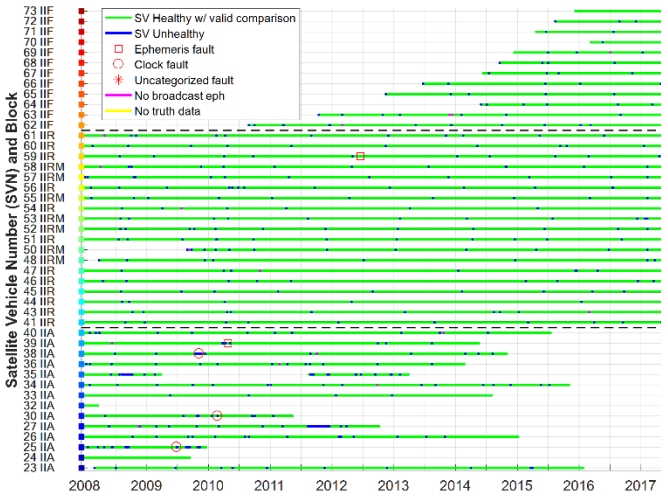

Figure 2: GPS constellation history overview, 2008-2017

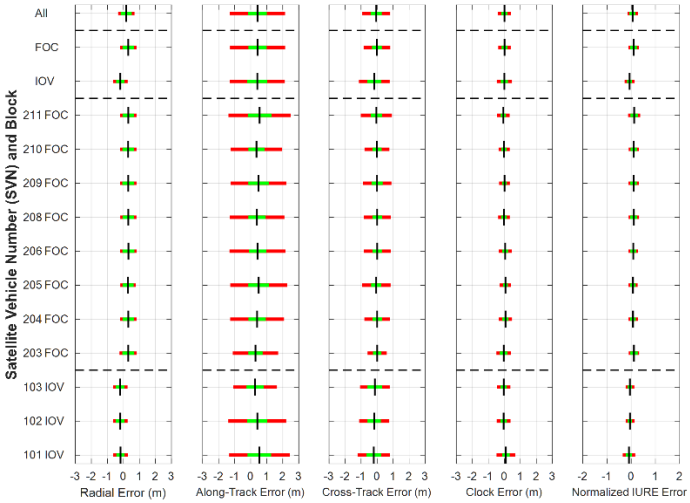

Figure 3: Galileo nominal statistics

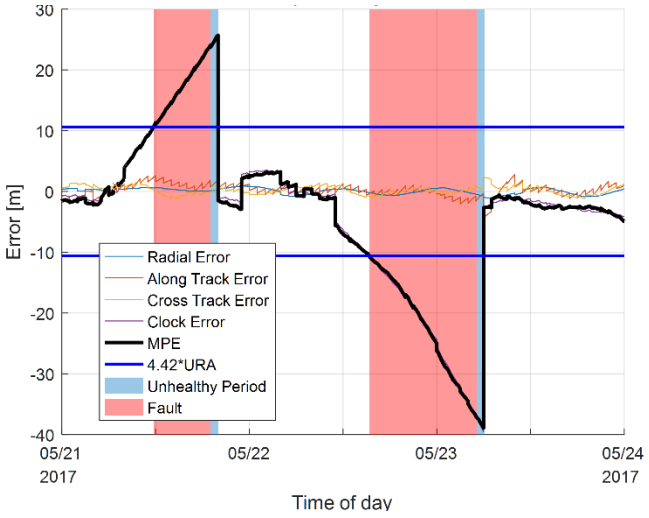

Figure 4: Example of broadcast clock/ephemeris anomaly observed in May 2017

Navigation message log threat and voting mitigation scheme

Erroneous entries in the navigation message logs used to produce the broadcast orbit and clock state are the most significant threat to the integrity of fault rate computations. The threat arises from errors in the logging of the navigation message at the receiver level, where what is recorded and stored in the IGS does not accurately reflect what was observed and used by the receiver. However, this is also a threat that can be significantly mitigated due to the large amount of redundancy in the stored data, as each navigation message is observed by anywhere from tens to hundreds of receivers at any given moment. The strategy, as described by Heng [11] and implemented here, is to aggregate as many receiver logs as possible then to clean and vote across the multitude of potential clock and ephemeris messages possible.

Figure 5 shows two BeiDou navigation message logs in RINEX format. Both messages are from PRN 12 on January 5, 2017 at 1:00:00. The two messages should match, but two common differences are highlighted. The top right example in Figure 5

highlights the type of small differences that occur commonly in the RINEX logs. The clock rate term is shown to be slightly different from one log to the next due to a slight truncation issue. This problem is mitigated in our process by, for each broadcast term, dividing by the scale factor used to produce the term in order to return to its integer form. The integer is rounded (typically the rounding error is extremely small), then the term is multiplied again by the scale factor to return to a float value that can be consistently compared across different receiver logs.

The bottom left example in Figure 5 demonstrates an issue that occurs more often in the RINEX navigation message logs of the newest constellations, Galileo and BeiDou, where parameters are not stored in a RINEX compliant manner, and the error is larger than simply rounding. The examples shows the TGD2 term in both cases, except one is not multiplied by the scale factor and is non-compliant with the RINEX format [12]. This type of error also commonly occurs in the Galileo SISA parameter, which is often reported as the index that is broadcast rather than the accuracy value in meters. Both of these types of errors can be fixed on a parameter by parameter basis, but are also more generally cleaned in the voting process. The screening and voting methods employed here not only improve the integrity of the fault statistics but also improve the confidence in them by producing additional information about the navigation messages used- in particular the number of stations that saw the exact message used and the number of stations that disagreed with the agreed-upon broadcast navigation message.

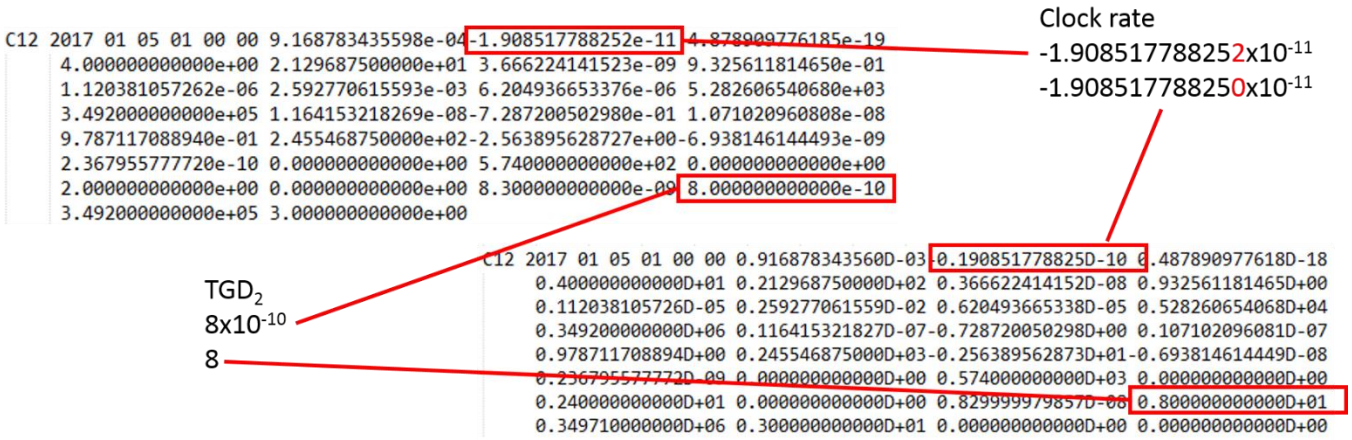

Figure 5: Example BeiDou navigation message logs in RINEX format from two different receivers

Missing precise clock and orbit products

When trying to carefully asses GNSS fault rates, erroneous or missing precise clock and orbit estimates are as harmful as erroneous or missing broadcast navigation messages. For example, of the five GPS fault events identified between 2008 and 2016, three of them would not appear if using the IGS final precise clock and orbit products, as the precise data was not available for those satellites during the faulted periods. Many of the periods where precise products are available are periods when anomalous behavior is observed by either the orbit or, as is more often the case, the clock. Because the behavior is anomalous, it seems that IGS analysis centers may be more inclined to simply not output a clock and orbit estimate during that period. Unfortunately, these are often the periods that are most important for anomaly investigation. In order to produce fault rate estimates with confidence, the analysis requires 100% availability of the fault detection system for satellites transmitting valid broadcast navigation messages, so when precise clock and orbit products are not available, an alternate method of fault detection must be employed.

The procedure used to detect faults when precise clock and orbit products are not available has been described previously by Gao [13] and used for extended GLONASS precise product outages [3], so only a brief description of the process will follow. The general process is shown in Figure 6. Broadly, one uses pseudoranges or carrier phase measurements from a receiver at a known location to estimate the contribution of the broadcast clock and ephemeris error to the user range error and determine whether or not a fault is present. First, given the a receiver with a precisely known position as well as multiple satellites in view with precisely known orbit and clock states, one can remove modellable effects from the pseudoranges, such as delays due to the ionosphere (using dual frequency measurements), troposphere, satellite clock bias, and geometric range.

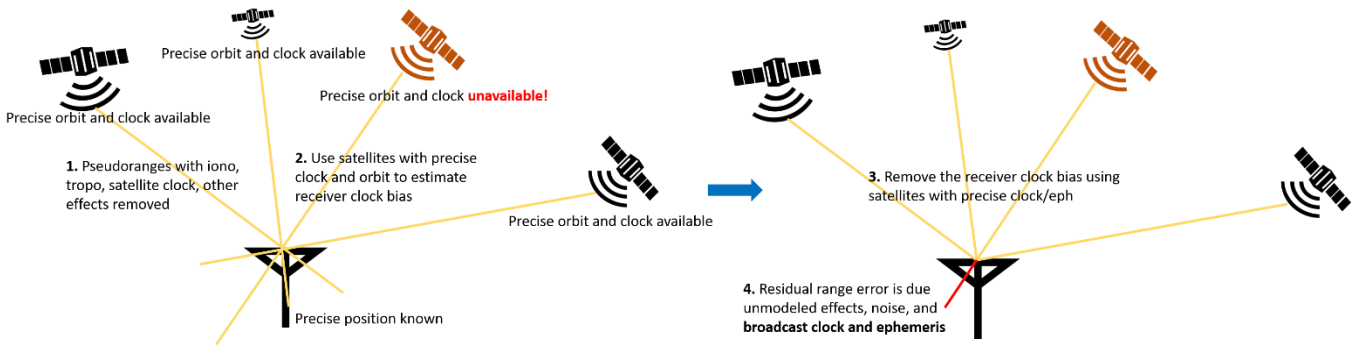

Figure 6: Fault detection for satellite with missing precise orbit and clock data

For the satellite of interest, which does not have precise clock and orbit available, the broadcast clock and orbit are used to produce the satellite clock bias and geometric range that are removed from the pseudorange. Once the modellable effects are removed, one can estimate the receiver clock bias from the pseudoranges of the satellites with precise clock and orbit products available and remove the estimated receiver clock bias from all of the pseudoranges. Finally, the residual error on the pseudorange of interest is then due to unmodelled effects, noise, and, in the case of a fault, primarily error from the broadcast clock and ephemeris. Given this estimate of the broadcast clock and ephemeris error for this single receiver, this process can be repeated across multiple receivers in view of the satellite of interest, and the aggregate can provide whether or not a fault was present.

Erroneous precise clock and orbit products

Even when precise clock and orbit products are available, inaccurate products can introduce false faults, again leading to inaccurate fault rate estimates. Figure 7 shows an example of erroneous precise clock estimates leading to what would be an incorrectly identified fault. The black line, again, represents the maximum projected error due to the broadcast clock and ephemeris, and the blue lines indicate the threshold for a fault. The red shading shows the period that is identified as a fault when using the standard procedure of comparing broadcast navigation messages to the precise clock and orbit products. From the standard procedure, it appears that a fault of greater than 350 meters persists for multiple hours. However, Figure 8 shows the signal to noise ratio (SNR) of the L1 C/A signal recorded from IGS receivers. The signal entirely drops out before the period of the previously described fault and does not return until the satellite is set unhealthy, which means that no fault could have been observed by a user, and so a fault did not occur.

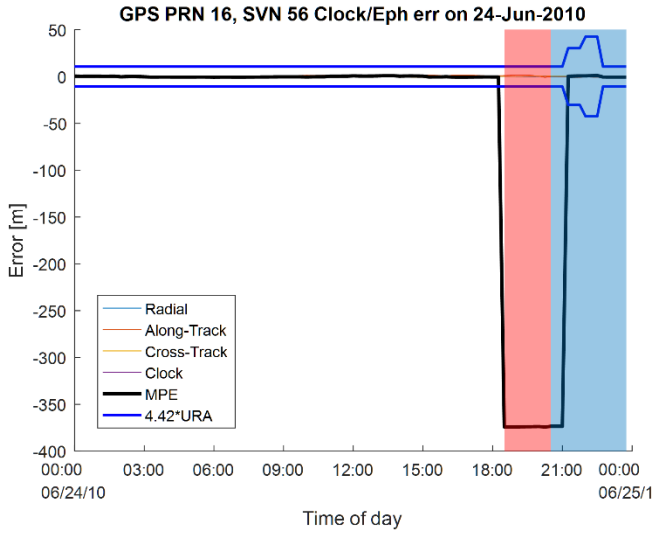

Figure 7: Example of erroneous precise clock data leading to false fault identification

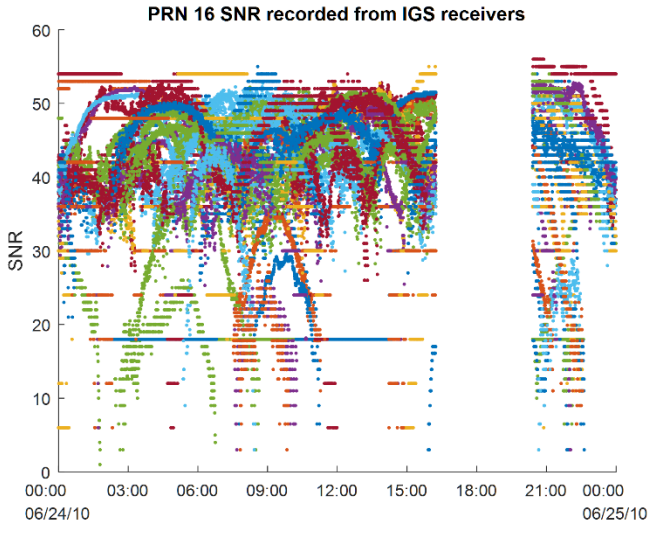

Figure 8: L1 C/A SNR during period of erroneous clock bias estimation

The standard process of comparing broadcast navigation data to externally produced precise clock and orbit products relies on those precise products to both be available but also accurate, and issues with either accuracy or availability can introduce significant errors in the computation of ISM parameters. In order to combat these issues, a system to independently verify the precise products is introduced and described in the following sections.

INDEPENDENT CLOCK BIAS ESTIMATION

Erroneous or missing precise clock products can impair our ability to identify faults and then confidently assess fault rates. Similarly, when only low rate clock products are available (either at 5 or 15 minute intervals), fault events can "hide" between the estimated epochs. For example, when the SISRE of a satellite jumps from small to large enough to be considered a fault if healthy in addition to being set from healthy to unhealthy at consecutive precise product estimate epochs, it is important to know exactly what happens in the transition, whether a fault occurred or the satellite was set unhealthy before the SISRE jumped. When only slower rate products are available, it is difficult to assess these transitions. Additionally, short fault events could exist between precise clock and orbit estimates that would not be observed through the normal process.

In order to mitigate these issues, we have developed a system to independently estimate GNSS clock states in order to both verify the externally produced precise clock products and to fill in periods where those estimates are not available, such as between intervals when only those low rate products are available. The goal of the Stanford University (SU) clock estimation is to increase the confidence in fault rate assessment process by producing a completely independent, verifiable precise clock product. This system gives us additional flexibility and confidence in the comparison of broadcast orbit and clock to precise estimates. Specifically, one advantage is that it allows us to estimate clock biases at the rate of our choice, only limited by observation rate. Our goal is to eventually estimate clock biases at 5 second intervals in order to verify the GPS six second time to alert. Independent clock estimation also allows one to evaluate the performance of different signal pairs. IGS products use the L1P-L2P observation pair, while aviation users will use the L1 C/A-L5 pair, the performance of which has not been evaluated over long periods. This clock estimation scheme will allow for the evaluation of the performance of any signal pairs of choice as well as the corresponding broadcast inter-signal corrections (ISC).

The performance goals of this estimation are different from those of the IGS analysis centers (AC), which have extremely high accuracy (~2.5 cm), but less than 100% availability. The accuracy goal of the SU clock estimates is approximately 0.5 meters 1-σ. The precise clock estimates will ultimately be compared against, in the case of GPS for example, a minimum URA of 2.4 meters and a minimum fault threshold of 10.6 meters, so centimeter level accuracy is not required. However, the ultimate goal of the SU estimation is to reach 100% availability of clock bias estimates- whenever the satellite is broadcasting a valid navigation signal, our desire is to be able to characterize its performance.

Filter overview

A Kalman filter (KF) is used to estimate the GNSS clock biases given precisely known satellite orbits and receiver positions. The KF was chosen for two primary reasons. First, it can be run continuously and thus does not suffer from the issue of misclosures at the boundaries between processing batches. Second, the processing time increases linearly with the number of epochs estimated, while this is often not the case for large batch processing cases, which makes the KF desirable for high estimation rates. It is notable that we are not estimating the satellite orbital states and instead only estimate the clock states. This is also for two reasons. Anomalous orbital events are rarer than clock events, and they typically occur more slowly than the clock events and thus are not in danger of being missed between estimation intervals, even for low estimation rates. Second, any errors in the precise orbit estimates will propagate into the clock estimates and eventually into the URE computations. Orbit errors will result in larger residuals on the receiver measurements because the orbit error will be projected differently onto different receivers, but they will nevertheless be estimated and visible. The clock estimation filter described here uses techniques and strategies from two previous works in particular by Hauschild [14] and Bock [15]. The initial goal of the SU filter is to use the produced clock estimates for verification of external precise clock products and fault detection. In the future, the goal will be to replace the external precise clock products entirely with the SU product and then use it for nominal error characterization as well as fault detection.

The observables used in the KF are ionosphere-free combinations of code and carrier phase ranges. Again, the exact signal pairs used are up to the user. In this paper, only preliminary verification results are shown, where the truth is taken to be IGS GPS precise clock estimates produced using the L1P-L2P signal pair, so the same pair is used here. The states estimated in the filter include the satellite clock bias (1 per satellite), satellite clock rate (1 per satellite), receiver clock bias (1 per receiver), float carrier phase ambiguity (1 per carrier phase arc), and tropospheric zenith-path-delay (1 per receiver). For the

approximately 60 receivers used, this typically results in approximately 800 states at each epoch, depending on the number of available observables. Because the KF estimates clock bias and clock rate, anomalous behavior such as large steps are not well estimated. Several strategies can be used to mitigate this, such as running the filter backwards again after the period and taking a weighted average of the two estimates based on the covariances. Another, more drastic strategy would be simply to use a batch least-squares process to estimate each clock state independent of the biases before or after. However, the KF is still adept at estimating clock biases during periods when the clocks exhibit nominal behavior, again, high accuracy estimation is not the ultimate goal of the SU filter.

Inputs

The Kalman filter requires four primary sets of inputs: station positions, differential code biases, phase center offsets and variations, and receiver measurements. The station positions are provided by the IGS and are centimeter-level accurate. However, IGS station position solutions are not always available. In this case, a PPP solution is produced and used instead. When comparing against another reference clock estimate, as is done in the results section of this paper, it is important that the observables used are consistent. IGS estimates use the L1P-L2P iono-free combination. The observables used in this filter are typically the L1 C/A-L2P combination, so IGS estimates of differential code biases are used to account for the timing offset between L1 C/A and L1P. In the future, the L1 C/A-L5 combination will be used. In this case, when evaluating the performance of the navigation message parameters, the broadcast inter-signal corrections must be applied, and the IGS differential code biases will not be necessary. The antenna phase center offsets and variations for both satellites and receivers are those produced by the IGS [16]. The measurement used in the KF are provided by 64 multi-GNSS receivers, which are a part of the MGEX receiver network. The receivers were chosen primarily for geographic diversity. Figure 9 shows the locations of the stations, and the colored shading indicates the number of receivers in view above each point at GPS altitude. There are enough stations in view of each point to provide significant redundancy, with the minimum number of receivers in view at any point of 11.

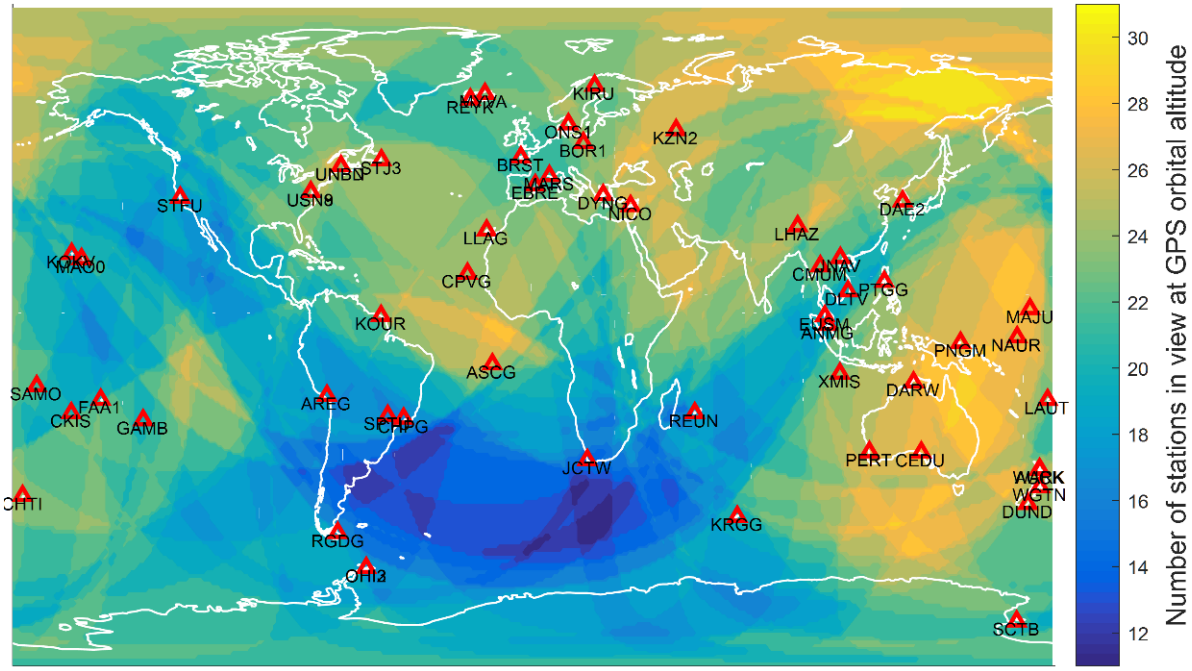

Figure 9: Receivers used in clock estimation Kalman filter. Shading indicates number of stations visible above that point at GPS altitude.

Structure

The Kalman filter is a commonly used estimation tool, so a detailed description of the KF will not be included, here, but some notes on the particulars of this specific implementation will be. The system begin by preprocessing observables. Cycle slips are detected, and short carrier phase arcs are removed. Additionally, a coarse estimate of the receiver clock bias is removed from all observables at each epoch. This is done because the receivers used use clocks of varying performance levels, and receiver clock bias jumps of up to 1 millisecond have been observed. Without removing the bulk of the receiver clock offset

at this step, large errors would be introduced by the receiver clock bias jumps. The station positions are then loaded from the IGS estimates when available. When unavailable, the PPP position solution is produced if necessary and simply loaded otherwise.

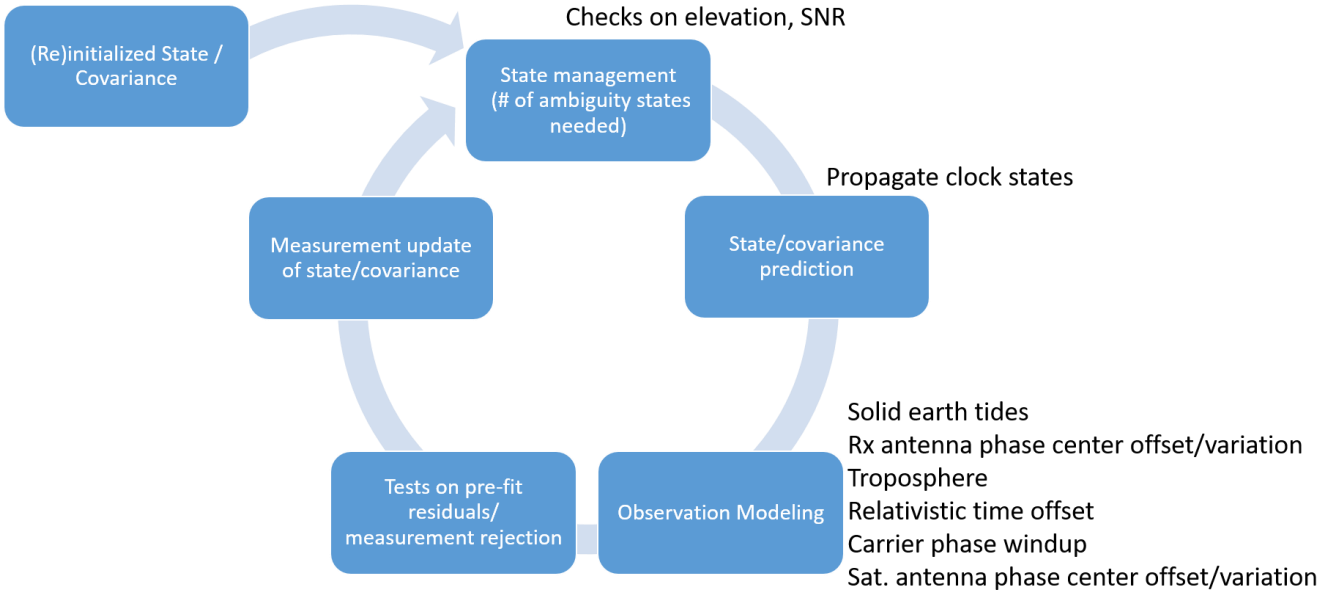

Figure 10: Clock estimation filter structure overview

An overview of the KF cycle is shown in Figure 10. The process begins by initializing the state and covariance matrix. If no previous data is available, the initial clock biases are initialized using the IGS final estimates, but this could be replaced with any other estimate including the broadcast state. If this is a continuation of a previous run of the filter, the state and covariance is loaded from that previously saved data. Entering the filter cycle, the first step is to examine which observables are available and to do carrier phase ambiguity state management. If a new carrier phase observable is available, then a new state needs to be added to the state vector and covariance matrix. Similarly, if a measurement has an insufficient signal to noise ratio or elevation angle from the receiver to the satellite, then if that state is not already included, it is ignored, otherwise it is removed. The time-update step of the KF is very simple, as most of the states are treated as stationary. The only exception is the clock bias, which is propagated forward by the clock rate.

In addition to the geometric range, the satellite clock bias, and the receiver clock bias, a number of other models go into observation modeling. In particular, solid Earth tides, receiver antenna phase offset and variation, tropospheric delay, relativistic time offset of the satellite clock, carrier phase windup, and satellite antenna phase center offset and variation are included. The tropospheric delay consists of a deterministic component as well as an estimated component to account for local conditions. Once the pseudoranges and carrier phases are modeled, they are compared to the actual measurements and screened for outliers. The screening process iterates through each station, performing a RAIM-like process by first checking the full set of measurements for outliers. If the RMS of the residuals exceed some threshold, then subsets are checked for consistency by removing measurements until a consistent set is found. This exclusion process is detailed in [14]. Those measurements that are excluded are then removed from the measurement set, and those carrier phase ambiguity estimates are reset at the next iteration. Finally, once the final measurement set is determined, the measurement update of the state and covariance can proceed, and the process is restarted at the next epoch.

RESULTS

Performance of the SU clock bias estimates is evaluated by measuring the difference between the SU estimates and the estimates from the Center for Orbit Determination European (CODE). CODE is an IGS analysis center and produces GPS clock bias estimates with ~2.5 cm accuracy at a 5 second rate. A specific run of the SU filter is evaluated here. The run uses data from a five day span from August 17, 2016 to August 22, 2016. Only GPS performance is evaluated, and the initial clock estimates are initialized with IGS precise clock estimates.

An overview of the clock bias difference between the SU and CODE clock bias estimates is shown in Figure 11. Each of the colored lines in the top plot of the figure represents the clock bias difference for a single satellite. The maximum error, after the initialization of the filter, of any single satellite in this period is 73 cm. The bottom plot in the figure shows the root-mean-squared difference across all satellites over time. The RMS error over the entire period is 18.5 cm. Overall, this performance is encouraging and sufficient for precise product verification and broadcast navigation message performance characterization. The RMS error of this systems is far below the 1-σ minimum URA for GPS of 2.4 meters. Even the a reduced URA of 1 meter that will come with CNAV can still be reliably characterized with this level of error, and faults, at 4.42 times the URA value, should also be able to be reliably detected.

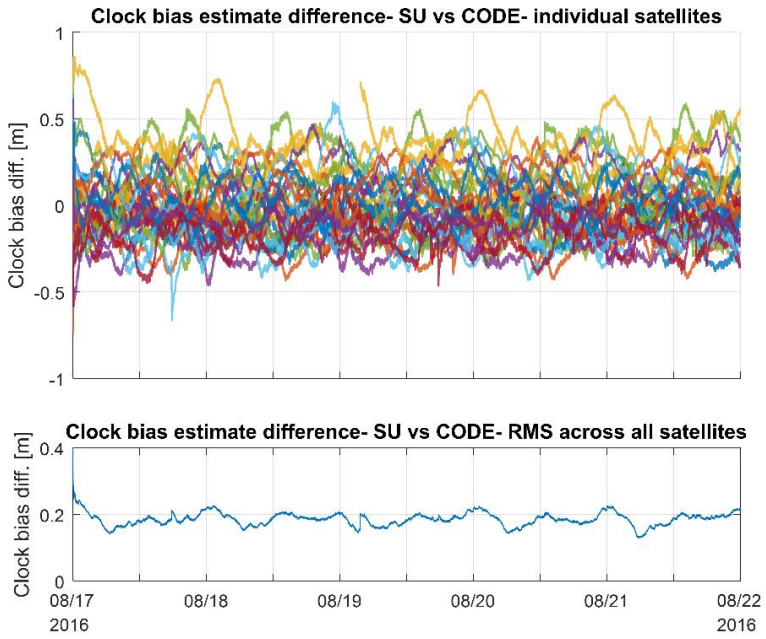

Figure 11: Clock estimation Kalman filter estimate performance overview. Top plot shows the difference between SU and CODE clock estimates for each SV. Bottom plot shows RMS of all errors at each epoch.

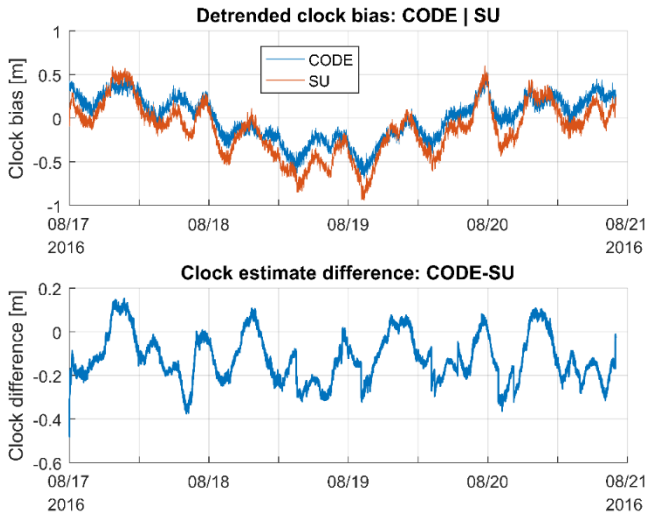

Figure 12: Clock bias estimates/difference for PRN 5, CODE vs SU

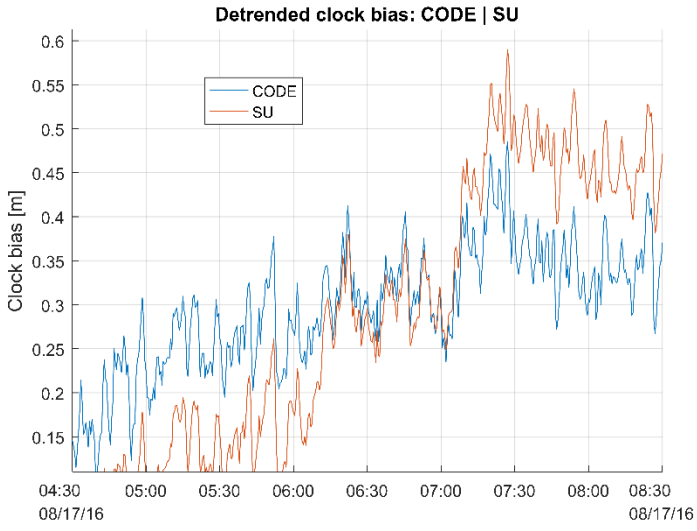

Figure 13: Zoomed in clock bias estimates for PRN 5, CODE vs SU

A closer examination of a comparison between the SU and CODE clock bias estimates for PRN 5 is shown in Figure 12 and Figure 13. The top plot in Figure 12 and Figure 13 show the two clock bias estimates with the mean constellation clock bias and a second-order polynomial removed. The same second-order polynomial line is removed from both estimates for visibility. The behavior of the clock is generally captured by the SU KF, and the lower plot in Figure 12, which shows the difference between the two clock estimates, shows that the difference between the two is fairly smooth and slowly varying. The slowly varying error appears to have a 24 hour period, corresponding to the GPS ground track repeat period. This may indicate an issue with a mis-modelling or missing model, which perhaps can be fixed. Figure 13 shows that the high-frequency content of the clock bias is well captured by the SU estimate due to the use of carrier phase measurements, and again, the error is slowly varying.

CONCLUSION AND WAY FORWARD

Multiple threats to the broadcast navigation message performance evaluation process have been identified, and several mitigation strategies have been described. The first threat described was to the broadcast navigation message logs themselves, where errors in the logging process at the IGS receiver level can introduce erroneous navigation message that were not actually broadcast by the satellites. The scrubbing and voting process was described, and some errors that particularly affect Galileo and BeiDou RINEX navigation message logs were identified. Threats to the overall process due to missing or erroneous precise orbit and clock data were also identified. A previously implemented method of identifying faults when there is no precise orbit and clock data available was described.

Finally, a Kalman filter-based precise clock bias estimator was described. The filter has been developed to improve the integrity of the fault-detection procedure by producing an independent estimate of GNSS clock biases that serves to both verify precise clock data when available and fill in when unavailable with the goal of 100% availability of precise clock estimates. In order to verify the performance of the filter, the clock bias estimates it produced have been compared to those produced by CODE during a period of nominal performance, which are centimeter-level accurate. The accuracy of the SU filter was shown to be <20 cm RMS over the verification period and is sufficient for our purposes.

Moving forward, a number of changes and improvements will come. The results presented in this paper were only for the GPS L1P-L2P combination as the first step in verifying the filter performance by comparing to another reference source. However, the final product must be multi-GNSS because ARAIM is necessarily multi-GNSS. We will also switch to evaluating the L1 C/A-L5 signal combination, as that is the signal pair that will be used in ARAIM receivers. General accuracy improvements will be sought, and the filter will be further stressed with anomalous clock behavior. In fact, anomalous clock behavior (discontinuities in clock bias or rate), may require that the estimation system be changed from a Kalman filter based design to a batch least squares based design. Finally, once the estimation system works in a satisfactory manner, it will be integrated into the daily processing and run over long periods.

ACKNOWLEDGMENTS

The authors would like to gratefully acknowledge the FAA Satellite Navigation Management Team for supporting this work under Cooperative Agreement 2012-G-003. The opinions expressed in this paper are the authors'.

REFERENCES

[1] T. Walter, J. Blanch, M. Joerger, and B. Pervan, "Determination of fault probabilities for ARAIM," in *2016 IEEE/ION Position, Location and Navigation Symposium (PLANS)*, 2016, pp. 451-461: IEEE.

[2] T. Walter and J. Blanch, "Characterization of GPS Clock and Ephemeris Errors to Support ARAIM," in *Proceedings of the ION 2015 Pacific PNT Meeting, Honolulu, Hawaii*, 2015, pp. 920-931.

[3] K. Gunning, T. Walter, and P. Enge, "Characterization of GLONASS Broadcast Clock and Ephemeris: Nominal Performance and Fault Trends for ARAIM," in *Proceedings of the 2017 International Technical Meeting of The Institute of Navigation, Monterey, California*, 2017, pp. 170-183.

[4] S. Perea Diaz, M. Meurer, M. Rippl, B. Belabbas, M. Joerger, and B. Pervan, "URA/SISA Analysis for GPS-Galileo ARAIM Integrity Support Message," 2015.

[5] Y. Wu *et al.*, "Long-term behavior and statistical characterization of BeiDou signal-in-space errors," *GPS Solutions*, pp. 1-16, 2017.

[6] O. Montenbruck, P. Steigenberger, and A. Hauschild, "Broadcast versus precise ephemerides: a multi-GNSS perspective," *GPS Solutions*, vol. 19, no. 2, pp. 321-333, 2015// 2015.

[7] Y. Feng and Y. Zheng, "Efficient interpolations to GPS orbits for precise wide area applications," *GPS Solutions*, vol. 9, no. 4, pp. 273-282, 2005.
[8] I. G. Service. *IGS Antenna Phase Center Offsets*. Available: ftp://igscb.jpl.nasa.gov/pub/station/general/igs08.atx
[9] O. Montenbruck *et al.*, "GNSS satellite geometry and attitude models," *Advances in Space Research*, vol. 56, no. 6, pp. 1015-1029, 9/15/ 2015.
[10] L. Heng, G. X. Gao, T. Walter, and P. Enge, "Statistical characterization of GLONASS broadcast clock errors and signal-in-space errors," in *Proceedings of the 2012 International Technical Meeting of the Institute of Navigation (ION ITM 2012), Newport Beach, CA*, 2012, pp. 1697-1707.
[11] L. Heng, "Safe Satellite Navigation with Multiple Constellations: Global Monitoring of GPS and GLONASS Signal-in-Space Anomalies," 2012.
[12] W. Gurtner and L. Estey, "RINEX-The receiver independent exchange format-version 3.00," *Astronomical Institute, University of Bern and UNAVCO, Bolulder, Colorado.*, 2007.
[13] G. X. Gao, H. Tang, J. Blanch, J. Lee, T. Walter, and P. Enge, "Methodology and case studies of signal-in-space error calculation: Top-down meets bottom-up," 2009.
[14] A. Hauschild, "Precise GNSS clock-estimation for real-time navigation and Precise Point Positioning," 2011.
[15] H. Bock, R. Dach, A. Jäggi, and G. Beutler, "High-rate GPS clock corrections from CODE: support of 1 Hz applications," *Journal of Geodesy*, vol. 83, no. 11, pp. 1083-1094, 2009.
[16] P. Rebischung and R. Schmid, "IGS14/igs14. atx: a new framework for the IGS products," in *AGU Fall Meeting 2016*, 2016.